Liquid Crystals
Publication details, including instructions for authors and subscription information:
http://www.informaworld.com/smpp/title~content=t713926090

Effect of the site of hydrogen-bonding on the liquid crystalline behaviour of supramolecular complexes

X. Y. Xu[a]; B. Y. Zhang[a]; L. X. Wang[a]; W. M. Gu[a]
[a] The Centre for Molecular Science and Engineering, Northeastern University, Shenyang, People's Republic of China

First published on: 01 October 2009

To cite this Article Xu, X. Y. , Zhang, B. Y. , Wang, L. X. and Gu, W. M.(2009) 'Effect of the site of hydrogen-bonding on the liquid crystalline behaviour of supramolecular complexes', Liquid Crystals, 36: 12, 1365 — 1372, First published on: 01 October 2009 (iFirst)
To link to this Article: DOI: 10.1080/02678290903247744
URL: http://dx.doi.org/10.1080/02678290903247744

Liquid Crystals,
Vol. 36, No. 12, December 2009, 1365–1372

Taylor & Francis
Taylor & Francis Group

Effect of the site of hydrogen-bonding on the liquid crystalline behaviour of supramolecular complexes

X.Y. Xu, B.Y. Zhang*, L.X. Wang and W.M. Gu

The Centre for Molecular Science and Engineering, Northeastern University, Shenyang 11004, People's Republic of China

(Received 3 September 2008; final form 10 August 2009)

Two series of hydrogen-bonded side-chain liquid crystal polymers have been prepared by mixing components containing carboxyl acid and pyridyl-based fragments. We have focused our attention on the effect that the position of the hydrogen bond donor or acceptor site attached to the side-chain backbone has on the hydrogen-bonding interactions and liquid crystalline phase transitions of the system. The liquid crystalline behaviour of the complexes is studied using Fourier transform infrared spectroscopy, differential scanning calorimetry, polarising optical microscopy and X-ray diffraction. The results indicate that the phase transition temperatures of the complexes are influenced by the site of hydrogen-bonding.

Keywords: pyridyl; carboxyl acid; hydrogen-bonding; liquid crystalline

1. Introduction

In recent years, liquid crystalline materials formed by self-assembling systems via a high degree of non-covalent interactions have attracted considerable attention due to their potential scientific and technological applications (*1–7*). The backbones of such self-assembling polymeric systems containing non-covalently attached moieties, in addition to covalently bonded units, impart reversibility and temperature sensitivity upon the system. Hydrogen-bonding is one of the most important interactions in chemical and biological processes and can be used to induce liquid crystallinity either in low molar mass organic compounds (*8, 9*), or in macromolecules. These systems are prepared using two suitably designed components that are commonly called H-bond donors and H-bond acceptors (*10–21*). Main-chain hydrogen-bonded liquid crystalline polymers are mostly based on bipyridyl and dicarboxylic acid fragments (*10–12*). Zuev and co-workers (*10*) described a linear supramolecular liquid crystalline polymer containing 4,4′-bipyridine and bis-(4-carboxyphenyloxycarbonyl) –heptanoate, and the kinetics of nematic nucleus growth in the melted polymer was studied. In the area of side-chain hydrogen-bonded liquid crystalline polymers (LCPs), pyridyl-based species have been non-covalently 'grafted' onto pendant aromatic acid units attached to preformed polymer chains (*6, 7, 13–21*). For example, Kato, Frechet *et al.* (*6, 7*) were particularly active in developing a large variety of supramolecular side-chain LCPs, generally utilising polymers with side-chains terminated by benzoic acid groups and small molecules containing pyridyl fragments such as stilbazole or bipyridine. Imrie and co-workers (*13–17*) reported three series of copolymers prepared by the reaction of a mesogenic methacrylate, 6-((4-((4-methoxyphenyl)azo)phenyl)oxy) hexyl methacrylate, with either 4-vinylpyridine, 2-vinylpyridine or styrene and these were blended with either a mesogenic acid, 6-((4-((4-methoxyphenyl)azo)phenyl)oxy)hexanoic acid, or a non-polar low molar mass liquid crystal, 4-(hexyloxy)-4′-methoxyazobenzene: Vuilluame and Bazuin described an ion-containing polyamphiphile, poly (ω-pyridylpyridinium dodecyl methacrylate) bromide complexed with 4-octylphenol by hydrogen bonding (*18*). Hydrogen bonding of the surfactant to the polymer was virtually complete up to near-equimolar phenol/pyridyl ratios. This is because, with the exception of ionic interactions, hydrogen bonding is the strongest of the non-covalent interaction forces between two molecules. The association between the 'donor' and 'acceptor' effectively induces hydrogen bonds that lead to a more stable structural organisation.

In this paper, we report the formation of side-chain liquid crystalline polymers through hydrogen bonding between pyridine and carboxylic acid fragments. As part of a programme aimed at investigating new supramolecular materials, here we focus our attention on the influence of differing the site on the side-chain backbone on the hydrogen-bonding interactions and LC phase transitions of this system. The thermal properties of these complexes are studied by fourier transform infrared spectroscopy (FTIR) spectra, differential scanning calorimetry (DSC), polarising optical microscopy (POM) and X-ray diffraction (XRD).

*Corresponding author. Email: baoyanzhang@hotmail.com

ISSN 0267-8292 print/ISSN 1366-5855 online

DOI: 10.1080/02678290903247744
http://www.informaworld.com

2. Experimental

2.1 Measurements

The FTIR spectra were measured on a Spectrum One (B) spectrometer (PerkinElmer, Foster City, CA). 1H NMR and 13C NMR spectra (300 MHz) were obtained with a Gemini 300 spectrometer (Varian Associates, Palo Alto, CA). Thermodynamic parameters were determined with a DSC 204 (Netzsch, Hanau, Germany) equipped with a liquid nitrogen cooling system. The heating and cooling rates were 10°C/min. A DMRX POM instrument (Leica, Germany) equipped with a THMSE-600 hot stage (Linkam, England) was used to observe phase transition temperatures and analyse liquid crystalline properties through the observation of optical textures. XRD measurements were performed with nickel-filtered Cu-K_a ($\lambda = 1.542$ Å) radiation with a DMAX-3A powder diffractometer (Rigaku, Tokyo, Japan).

2.2 Monomer synthesis

2.2.1 4-pyridine-4′-methylbenzoate (p-1), 4-pyridine-4′-methoxybenzoate (p-2), 4-pyridine-4′-ethoxybenzoate (p-3)

The p-1, p-2, and p-3 monomers were synthesised using the same method. An example is presented below. p-Toluoylbenzoyl chloride was synthesised through the reaction of 4-methylbenzoic acid with excess thionyl chloride according to the method reported by Hu *et al.* (*22*). p-Toluoylbenzoyl chloride (0.05 mol) was then added dropwise to a solution of 4-hydroxypyridine (5.7 g, 0.06 mol) in 50 ml of tetrahydrofuran (THF) and 20 ml of pyridine under quick stirring. The reaction mixture was refluxed for 8 h. After the removal of the excess solvent, the rest was poured into excess water and neutralised with dilute hydrochloric acid. The crude product was obtained by filtration and washed with water to remove unreactive 4-hydroxypyridine. The white solid was obtained by recrystallisation with ethanol. Yield: 74%. Mp: 111.2°C. IR (KBr): 2921 (CH_3–), 1746 (C=O), 1609–1484 (Ar–), 1587 (pyridine). ^{1}H NMR (CDCl3) δ: 2.37(t, 3H, C**H**$_3$–); 7.16–7.74 (m, 4H, Ar–***H***); 7.26–8.57 (s, 4H, pyridine-***H***). ^{13}C NMR (CDCl3) δ: 20.9 (1C, pert. C); 164.0(1C, C=O); 116.4, 129.1, 130.2, 151.2 (8C, tert. C); 127.6, 142.9, 159.8 (3C, quat. C). Elemental analysis: calculated for $C_{12}H_{11}NO_2$, C 71.64, H 5.47; found, C 72.16, H 5.41%.

2.2.2. Hexanedioic acid monocholesteryl ester (c-4) and sebacylic acid monocholesteryl ester (c-5)

Using the same method, hexanedioic acid monocholesteryl ester (c-4) and sebacylic acid monocholesteryl ester (c-5) were synthesised according to a procedure reported elsewhere (*23*), which is shown in Scheme 1.

2.2.3 1-pyridine-6-cholesteryl-adipate (p-4), 1-pyridine-6-cholesteryl-sebacate (p-5)

The 1-pyridine-6-cholesteryl-adipate (p-4) and 1-pyridine-6-cholesteryl-sebacate (p-5) were synthesised by the same method. An example is presented below. In order to obtain p-4, the c-4 chloride (2.675 g, 0.05 mol), obtained from the reaction of c-4 and excess thionyl chloride, was dissolved in 20 ml chloroform, and added dropwise to a solution of 4-hydroxypyridine (5.7 g, 0.06 mol) in 50 ml of THF and 20 ml of pyridine under quick stirring. The reaction mixture was refluxed for 8 h. After the removal of the excess solvent, the rest was poured into excess water and neutralised with dilute hydrochloric acid. The crude product was obtained by filtration and washed with water to remove unreactive 4-hydroxypyridine. The white solid (p-4) was obtained by recrystallisation with ethanol and dried in vacuum. Yield: 67%. Mp: 112.2°C. IR (KBr): 2928 (CH_3–), 1742 (C=O), 1611–1482 (Ar–), 1581 (pyridine). ^{1}H NMR (CDCl3) δ: 1.58–2.27(m, 8H, –C**H**$_2$–); 5.41 (m, 1H, =C**H**– in cholesteryl); 3.87 (m, 1H, in cholesteryl); 1.21–2.03 (m, 43H, **H**-cholesteryl); 7.24–8.54 (m, 4H, **H**-pyridine). ^{13}C NMR (CDCl3) δ: 18.6, 21.3, 21.3, 22.8, 22.8 (5C, methyl-C in cholesteryl); 21.7, 21.9, 22.1, 22.7, 28.7, 30.6, 31.9, 35.4, 38.9, 39.4, 40.2 (11C, pert. C in cholesteryl); 28.1, 29.8, 30.2, 42.8, 46.2, 48.8, 50.7, 121.6 (8C, tert. C in cholesteryl); 39.6, 40.9, 148.2 (3C, quat. C in cholesteryl); 25.2, 25.1, 32.6, 32.9 (4C, pert. C); 169.2, 172.4 (2C, C=O); 120.6, 120.6, 152.6, 152.6, 160.5 (5C, C in pyridine). Elemental analysis: calculated for $C_{38}H_{57}O_4N$, C 77.16, H 9.64; found, C 77.28, H 9.51%.

2.3 Polymer synthesis

For the synthesis of polymers P-C and P-P, the same method was used, which is shown in Scheme 1. 4-(Allyloxy) benzoic acid (I) and 4-pyridine-4-allyloxybenzoate (II) were synthesised according to a procedure reported elsewhere (*24, 25*).

2.4 Complexes formation

Hydrogen-bonding complexes were prepared by simply mixing the two components, the proton donor and acceptor, with exact 1:1 stoichiometry in THF, followed by stirring for 12 h. THF was removed at 60°C, and the resulting solid was then dried in a vacuum at 60°C. The structures of monomers and complexes are shown in Scheme 2.

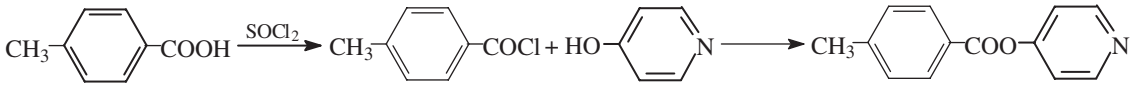

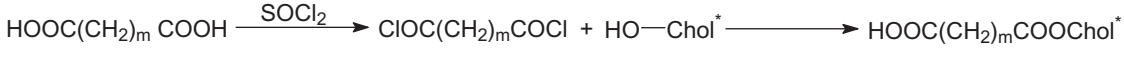

c-4: m=4; c-5: m=8

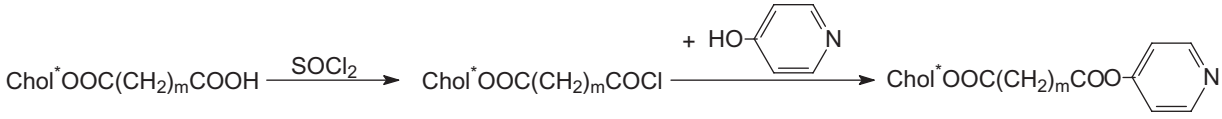

p-4: m=4; p-5: m=8

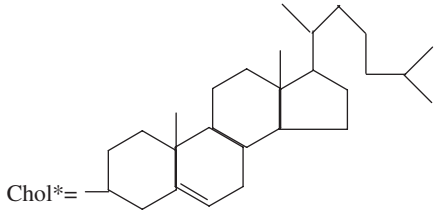

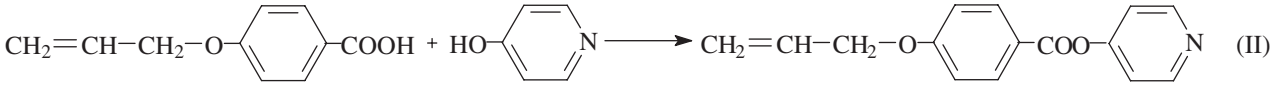

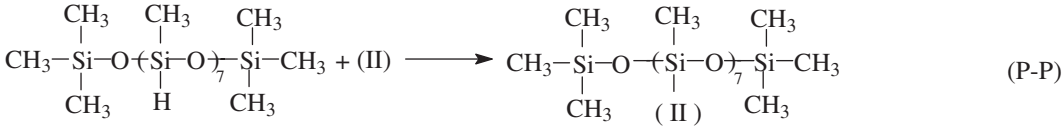

(P-P)

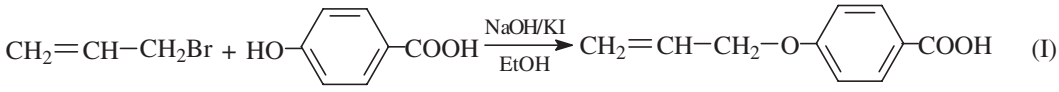

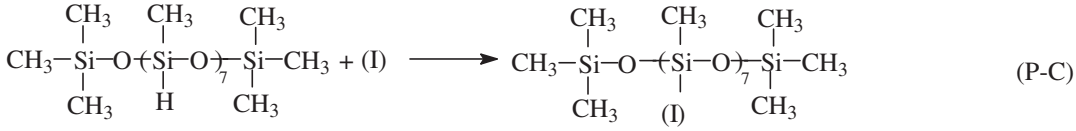

(P-C)

Scheme 1. Synthesis routine of p-1, p-4, c-4, P-C, and P-P.

3. Results and discussion

3.1 Spectroscopic analysis

The FTIR spectra of the acceptor, the donor and the hydrogen-bonded complexes are shown in Figure 1. The proton donor (P-P) forms an acid dimer that exhibits a broad O-H band from 3250 to 3600 cm^{-1} and C=O bands at about 1690 and 1730 cm^{-1}. In contrast, the FTIR spectra for both the hydrogen-bonded complexes, for example, P-C/p-2 and P-P/c-5, showed two new bands centred at about 2510 and 1920 cm^{-1} but did not contain the broad peaks from 3250 to 3600 cm^{-1}, which

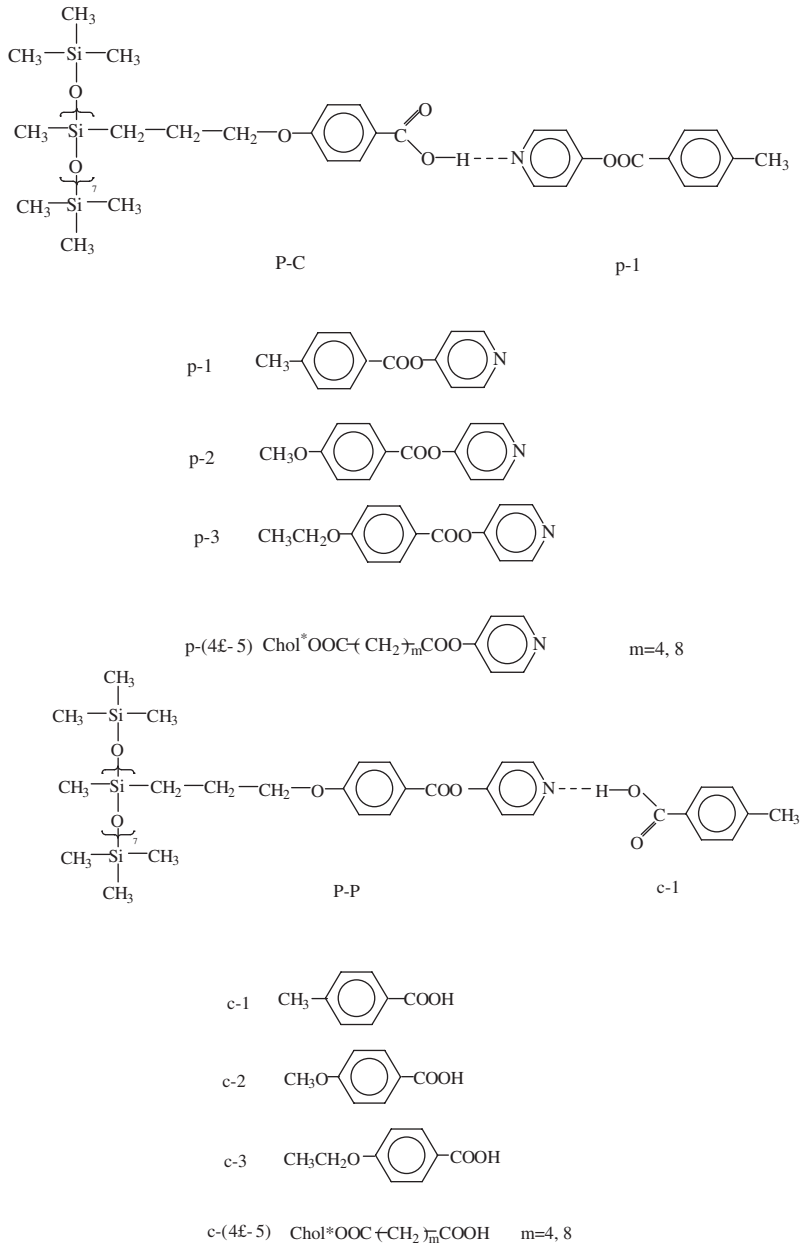

Scheme 2. The structure of monomers and complexes.

suggests the absence of the acid dimer in the complexes. Therefore, these new absorption bands are assigned to the hydrogen-bonding interaction between the carboxylic acid and the pyridine fragments, i.e. O-H···N. The results from the FTIR spectra clearly indicate that intermolecular hydrogen bonding does exist in the complexes. Hydrogen bonds have a major impact on the vibrational properties of hydrogen-bonding groups and so FTIR spectroscopy is well suited for the study of the influence of hydrogen bonding during mesophase formation and isotropisation (*26, 27*).

3.2 Thermal properties of supramolecular complexes

P-P exhibited a nematic phase, p-4, p-5, c-4 and c-5 exhibited the cholesteric phase, while the other proton acceptors and proton donors did not exhibit any mesomorphic behaviour. The phase transition temperatures of all the monomers are shown in Table 1. Most complexes displayed mesogenic behaviours and multiple phase transitions on heating and cooling, indicating the formation of liquid crystalline phases. The phase transitions of the complexes were studied using DSC in combination with POM, and the transitional properties are summarised in Tables 2 and 3.

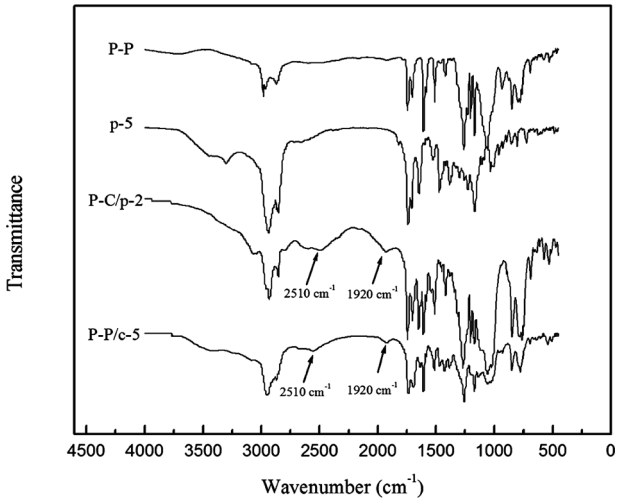

Figure 1. The Fourier transform infrared spectroscopy spectra of P-P, p-5, P-C/p-2, and P-P/c-5.

Table 1. Thermal transition data of the monomers.

	Thermal transitions, °C (corresponding enthalpy change, J/g) from DSC	
Monomer	Heating	Cooling
c-1	Cr 187.6 (148.5) I	I 169.8 (94.9) Cr
c-2	Cr 191.5 (82.3) I	I 167.4 (68.9) Cr
c-3	Cr 203.4 (184.4) I	I 189.8 (26.44) Cr
c-4	Cr 127.5 (44.5) N*143.4 (1.53) I	I 139.5 (2.64) N* 73.4 (27.3) Cr
c-5	Cr 119.8 (31.1) N* 123.4 (1.24) I	I 118.6 (4.27) N* 98.3 (40.3) Cr
p-1	Cr 111.8 (106.4) I	I 93.4 (38.9) Cr
p-2	Cr 102.5 (62.7) I	I 74.5 (32.4) Cr
p-3	Cr 94.2 (104.9) I	I 73.4 (62.4) Cr
p-4	Cr 112.2 (52.6) N*145.8 (1.59) I	I 130.5 (2.36) N* 86.4 (38.3) Cr
p-5	Cr 103.6 (30) N* 119.3 (3.11) I	I 117 (2.9) N*66.2 (15.5) Cr

DSC, differential scanning calorimetry; Cr, crystalline; N, nematic; N*, chiral nematic; and I, isotropic.

Table 2. Thermal transition data of P-C/p-n complexes obtained from DSC and POM analysis.

	Thermal transitions, °C (corresponding enthalpy change, J/g) from DSC [a]		Thermal transition(°C) from POM [b]	
Complex	Heating	Cooling	Heating	Cooling
P-P	G -13.2 Cr 67 N 109 (1.36) I	[c]	Cr 71 N 112 I	I 110 N 67 Cr
P-P/c-1	G -6.2 Cr 76 N 114 (2.98) I	I 75 N 64 (1.09)Cr	Cr 80 N 110 I	I 82 N 53 Cr
P-P/c-2	G -5.6 Cr 100 N 146 (1.68) I	[c]	Cr 102 N 152 I	I 138 N 67 Cr
P-P/c-3	G 1.5 N 142 (2.08) I	[c]	Cr 102 N146 I	I 146 N 59 Cr
P-P/c-4	G 7.6 Cr 112(4.09) N*	I 100 N*	Cr 108 N* 120 I	I 115 N* 43 Cr
P-P/c-5	G -5.4 Cr 75 N*102 (2.16) I	N*88 Cr	Cr 84 N*112 I	I 106 N* 79 Cr

DSC, differential scanning calorimetry; POM, polarising optical microscopy; G, glass transition temperature; Cr, crystalline; N, nematic; N*, chiral nematic; and I, isotropic.
a, Data were obtained from the second scan; b, Heating and cooling rates 5°C min^{-1}.
c, No observed; d, No mesophase.

Table 3. Thermal transition data of P-P/C-n complexes obtained from DSC and POM analysis.

	Thermal transitions, °C (corresponding enthalpy change, J/g) from DSC [a]		Thermal transition °C from POM [b]	
Complex	Heating	Cooling	Heating	Cooling
P-C	G 15 Cr 121 I	[c]	[d]	[d]
P-C/p-1	G 0.3 Cr 81 (3.26) N	N 47 (0.96) Cr	Cr 79 N 104 I	I 97 N 52 Cr
P-C/p-2	G 2.8 Cr 87 N119 (1.69) I	[c]	Cr 76 N 122 I	I 94 N 51 Cr
P-C/p-3	G 3.8 Cr117 N 164 (2.98) I	I 122N 55 (1.35) Cr	Cr 114 N 165 I	I 121 N 50 Cr
P-C/p-4	G 9.2 Cr 140 (3.68) N*	[c]	Cr 145 N*160 I	I 142 N* 46 Cr
P-C/p-5	G 8.4 Cr 77 N*106 (0.96)I	N* 79 Cr	Cr 65 S 90 N*110 I	N* 65 Cr

DSC, differential scanning calorimetry; POM, polarising optical microscopy; G, glass transition temperature; Cr, crystalline; N, nematic; N*, chiral nematic; and I, isotropic.
a, Data were obtained from the second scan; b, Heating and cooling rates 5°C min^{-1}.
c, No observed; d, No mesophase.

The glass transition temperature (T_g) and the melt transition (T_m) for P-C/p-1, P-C/p-2, and P-C/p-3 increased gradually on increasing the length of the spacer in the proton acceptors. For example, the T_m for complexes P-C/p-1, P-C/p-2, and P-C/p-3 increased from 81 to 117°C, while the length of the spacer in the acceptors increased from methyl to oxyethyl. Similarly, the T_g of these complexes increased on increasing the spacer length in the proton acceptors. This is because the terminal groups of the proton acceptors change from methyl to oxyethyl, which inhibits the movement of the side-chain backbone of the complexes. The effect of lengthening the terminal group in proton acceptors leads to the increase in the transition temperatures. On the other hand, the T_m for P-C/p-4 and P-C/p-5 decreased from 140 to 77°C with the length of the spacer in the proton acceptors increasing from four to eight alkyl units. Similarly, T_g of the complexes P-C/p-4 and P-C/p-5 decreased

on increasing the spacer length in the proton acceptors. This is because the decrease in rigidity can be offset by replacing four with eight alkyl units, and the T_g or T_m of P-C/p-5 are dominated by the more flexible proton acceptors p-5 compared with P-C/p-4, which leads to the decrease in the transition temperatures.

Similar to the behaviour of T_g and T_m of the P-C/p-ns complexes, T_g and T_m of P-P/c-1, P-P/c-2, and P-P/c-3 increased on increasing the spacer length in the proton donors. Moreover, T_g and T_m of the complexes P-P/c-4 and P-P/c-5 decreased on increasing the spacer length in the proton donors.

Compared with P-P/c-ns, the phase transition temperatures of P-C/p-ns are greater. For example, the T_g of P-C/p-1 and P-P/c-1 were 0.3 and -6.2°C, and the T_m of P-C/p-1 and P-P/c-1 were 81 and 76°C, respectively. This is due to the hydrogen bonding differing at the site of side attached to the polymer side chain in the complexes. That is, as the fragment associated with hydrogen bonding on the side-chain becomes larger, movement of the molecular chains becomes more difficult, which consequently makes complex formation more difficult.

3.3 Optical properties

P-C/p-1, P-C/p-2, P-C/p-3, P-P/c-1, P-P/c-2, and P-P/c-3 showed characteristic nematic textures. Figure 2(a) shows a threaded texture exhibited by P-C/p-1 obtained on heating to the nematic melt at 90°C. Figure 2(b) shows the spherulitic texture of P-P/c-2, obtained on cooling from the nematic melt. For P-C/p-4, P-C/p-5, P-P/c-4, and P-P/c-5 complexes, chiral nematic phases with a characteristic oil texture and broken focal-conic fans could be clearly seen using POM as shown in Figure 2(c) and 2(d), respectively.

3.4 X-ray diffraction analysis

The complexes were quenched to room temperature from temperatures within the liquid crystal phase,

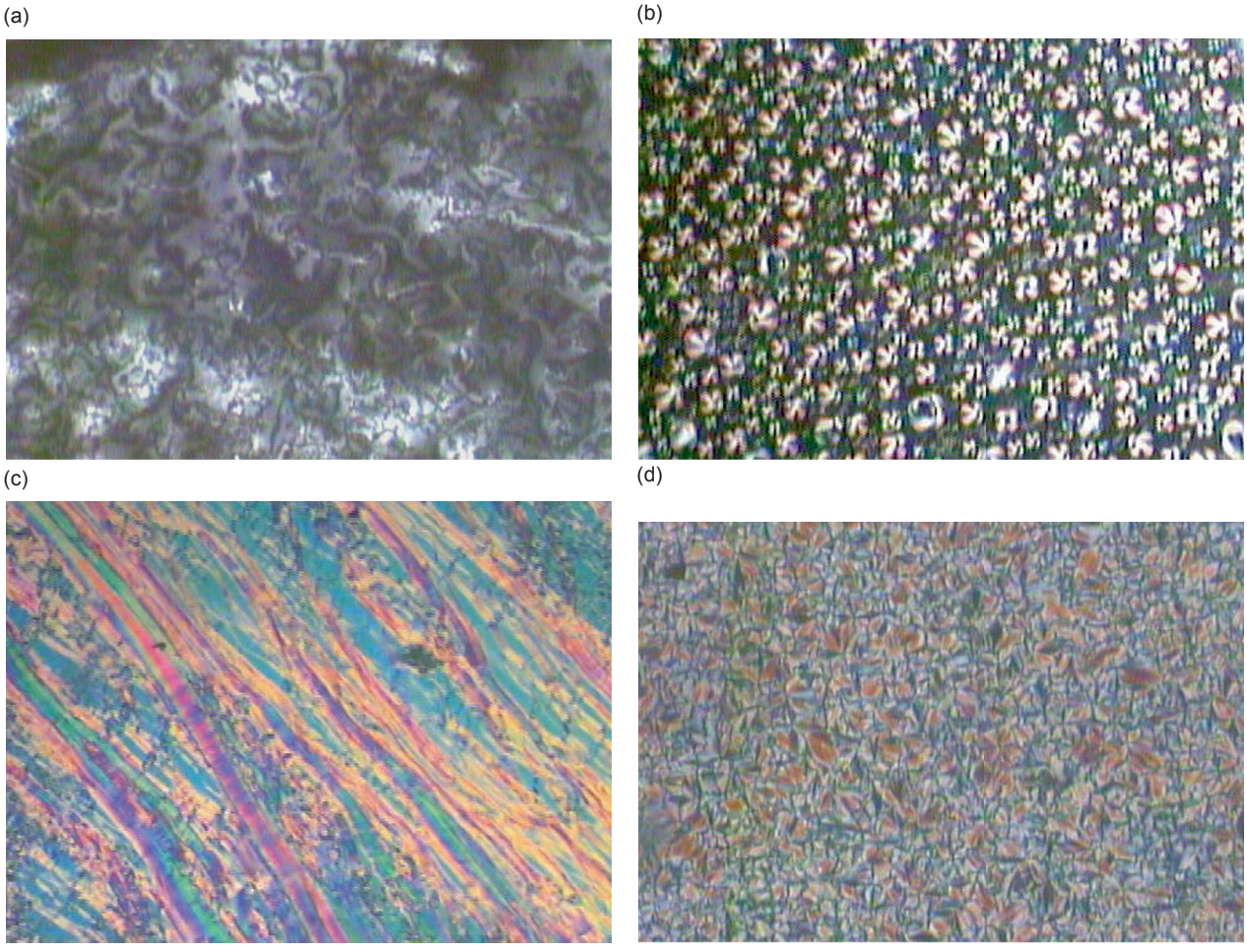

Figure 2. Polarising optical microscopy of complexes (a) P-C/p-1, (b) P-P/c-1, (c) P-C/p-4, and (d) P-P/c-5.

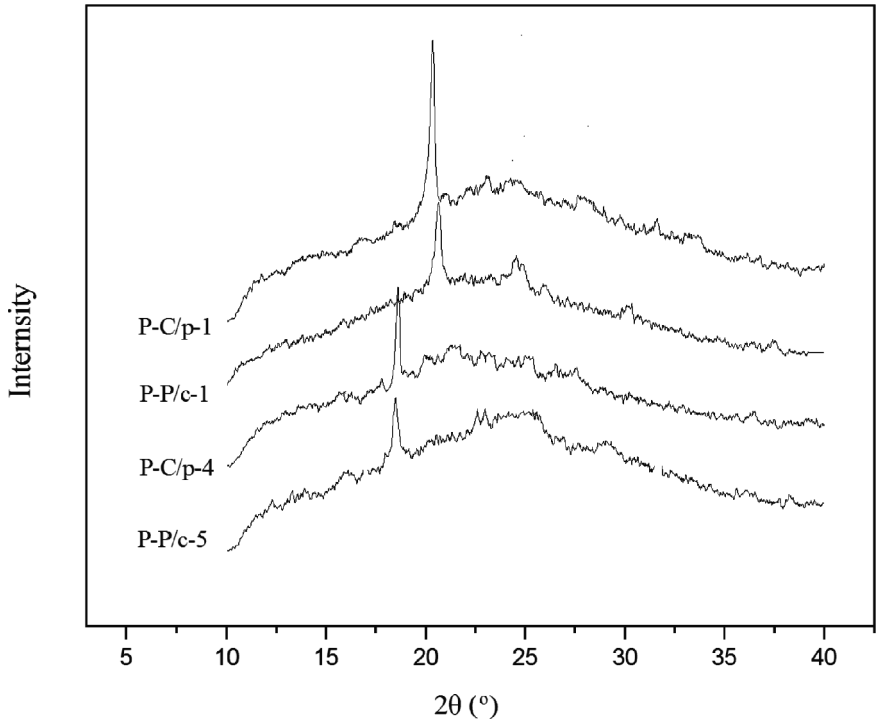

Figure 3. X-ray diffraction pattern of complexes P-C/p-1, P-P/c-1, P-C/p-4, and P-P/c-5.

and subjected to XRD experiments. The X-ray diffractograms of the complexes P-C/p-1, P-P/c-1, P-C/p-4, and P-P/c-5 are shown in Figure 3. The small-angle region for all the complexes showed no reflections. In the wide-angle region, a reflection corresponding to $2\theta \approx 20^\circ$ was seen; the complexes P-C/p-1 and P-P/c-1 showed similar XRD results, indicating the formation of a nematic phase. For complexes P-C/p-4 and P-P/c-5, a sharp scattering at 16–18° (2θ) appeared which is characteristic of a chiral nematic phase. The XRD results of complexes P-C/p-4 and P-P/c-5 are consistent, therefore, with the chiral nematic phase assignment based on the oil textures as shown in Figure 3(c) and (d).

4. Conclusions

In this paper, we synthesised two series of hydrogen-bonded liquid crystalline complexes by mixing components containing carboxyl acid and pyridine fragments. The effects of the site of hydrogen bonding attached to the side-chain backbone on phase transition temperatures have been investigated. The results showed that increasing the length of the terminal group in proton donors or proton acceptors resulted in the phase transition shifting to a higher temperature.

Acknowledgements

The authors are grateful to National Science Fundamental Committee of China, and HI-Tech Research and development program (863) of China.

References

(1) Kato, T. In *Handbook of Liquid Crystals* (1998); Demus, D., W.Goodby, J., Gray, G.W., Spiess, H.W.V. Eds.; Wiley-VCH: Weinheim, 2B: 969 and references therein.
(2) Sijbesma, R.P.; Beijer, F.H.; Brunsveld, L.; Folmer, J.B. *Science*, **1997**, *278*, 1601–1604.
(3) Burke, K.A.; Sivakova, S.; Mckenzie, B.M.; Mather, P.T.; Rowan, S.J. *J. Polym. Sci.: Part A: Polym. Chem.*, **2006**, *44*, 5049–5059.
(4) Reinhoudt, D.N.; Crego-Calama, M. *Science* **2002**, *295*, 2403–2407.
(5) Lehn, J.M. *Superamolecular Chemistry-Concepts and Perspectives*; VCH: Weinheim, 1995.
(6) Kato, T.; Kihara, H.; Ujiie, S.; Uryu, T.; Frechet, J.M.J. *Macromolecules* **1996**, *29*, 8734–8739.
(7) Kato, T.; Kihara, H.; Kumar, U.; Uryu, T.; Frechet, J.M.J. *Angew. Chem., Int. Ed. Engl.* **1994**, *33*, 1644–1645.
(8) Kohlmeier, A.; Janietz, D. *Liq. Cryst.* **2007**, *34*, 65–71.
(9) Krowczynski, A.; Trzcinska, K.; Gorecka, E.; Pociecha, D. *Liq. Cryst.* **2008**, *35*, 143–147.
(10) Zuev, V.; Bronnikov, S. *Liq. Cryst.* **2008**, *35*, 1293–1298.
(11) Toh, C.L.; Xu, J.; Lu, X.; He, C. *Liq. Cryst.* **2008**, *35*, 241–251.

(12) Bhowmik, P.K.; Wang, X.B.; Han, H.S. *Liq. Cryst.* **2007**, *34*, 841–854.
(13) Stewart, D.; Imrie, C.T. *Macromolecules* **1997**, *30*, 877–884.
(14) Stewart, D.; Imrie, C.T. *Liq. Cryst.* **1996**, *20*, 619–625.
(15) Stewart, D.; Imrie, C.T. *J. Mater. Chem.* **1995**, *5*, 223–228.
(16) Alder, K.I.; Stewart, D.; Imrie, C.T. *J. Mater. Chem.* **1995**, *5*, 2225–2228.
(17) Wallage, M.J.; Imrie, C.T. *J. Mater. Chem.* **1997**, *7*, 1163–1167.
(18) Vuillaume, P.Y.; Bazuin, C.G. *Macromolecules* **2003**, *36*, 6378–6388.
(19) Bazuin, C.G.; Brodin, C. *Macromolecules* **2004**, *37*, 9366–9372.
(20) Kawakami, T.; Kato, T. *Macromolecules* **1998**, *31*, 4475–4479.
(21) Kato, T. *Supramol. Sci.* **1996**, *3*, 53–59.
(22) Hu, J.S.; Zhang, B.Y.; Liu, Z.J.; Zang, B.L. *J. Appl. Polym. Sci.* **2001**, *80*, 2335–2340.
(23) Yao, D.S.; Zhang, B.Y.; Zhang, W.W.; Tian, M. *J. Mol. Struc.* **2008**, *881*, 83–89.
(24) Xu, H.; Kang, N.; Xie, P. *Liq. Cryst.* **2000**, *27*, 169–176.
(25) Hu, J.S.; Zhang, B.Y.; Sun, K. *Liq. Cryst.* **2003**, *30*, 1267–1275.
(26) Lin, H.C.; Lin, Y.S.; Chen, Y.T.; Chao, I.; Li, T.W. *Macromolecules* **1998**, *31*, 7298–7311.
(27) Barmatov, E.B.; Obrascov, A.A.; Pebalk, D.A.; Barmatova, M.V. *Coll. Polym. Sci.* **2004**, *282*, 530–534.